The scattering of electrons from inert gases. II. Absolute differential elastic cross sections for neon, krypton and xenon atoms

J. Phys. B: Atom. Molec. Phys., Vol. 8, No. 13, 1975. Printed in Great Britain.

The scattering of electrons from inert gases II. Absolute differential elastic cross sections for neon, krypton and xenon atoms

J F Williams and A Crowe

Department of Pure and Applied Physics, The Queen's University of Belfast, Belfast BT7 1NN, Northern Ireland

Received 26 March 1975, in final form 5 May 1975

Abstract. Measurements of the absolute differential cross sections for the elastic scattering of electrons from neon, krypton and xenon for a wide range of electron energies and scattering angles and with high angular resolution are presented. The range of electron energies is 20 to 400 eV, the range of scattering angles from 20 to 150 degrees and the angular resolution of both the incident and scattered electron beams is 1·5 degrees.

The experimental method is based on the crossed electron and modulated atom beams techniques. Measured angular distributions have been made absolute by carrying out phaseshift analyses over the 19·35 eV $(1s2s^2)^2S$ resonant state of helium and the 11·10 and 11·27 eV $(3s^23p^54s^2)$, $^2P_{1/2}$, $^2P_{3/2}$ resonance doublet in argon coupled with accurate determinations of the beam density ratios of neon, krypton and xenon to helium and argon. The measured angular distributions agree best with the recent high angular resolution data of Lewis *et al.* The absolute differential cross sections are not consistently in agreement with any previous absolute determinations. There is good general agreement with the relativistic exchange calculations of Walker, but there is considerable disagreement, particularly in the case of xenon, with the optical-model calculations of Lewis *et al.*

1. Introduction

Although we are now in the midst of the second period of intense activity as regards the experimental measurement of differential elastic scattering cross sections for electrons from the rare-gas atoms, there is still a great need for high quality absolute data. The first period of intense activity took place in the early 1930's and concentrated on the measurement of relative cross sections, ie angular distributions. These early data have been compiled graphically by Kieffer (1971) and discussed by Massey and Burhop (1969).

Recent data (since 1967) still suffers from at least one of the following disadvantages. (i) The cross sections are not truly absolute, being either relative or normalized to some theoretical model or other absolute data. (ii) The angular resolution of the apparatus is insufficient to completely resolve sharp angular variations in the cross sections. (iii) Limited energy and angular ranges are considered. This restriction limits the value of the results as a means of testing various theoretical models.

In the case of elastic scattering of electrons from helium no pronounced structure is likely in the differential cross section and hence the second condition, (ii), can be relaxed

somewhat. A number of absolute differential elastic scattering cross section measurements have been reported over various energy and angular ranges in helium. Nevertheless, to our knowledge, no single experiment completely satisfies condition (iii).

For argon, the above criteria are only satisfied by recent work from this laboratory (Williams and Willis 1975a). In view of the fact that the above conditions have not previously been satisfied for neon, krypton and xenon, the purpose of the present paper is to present the results of an extension of the argon work to include these species. The data were obtained using the crossed electron and modulated atom beams technique. The measured angular distributions are converted into absolute differential cross sections by carrying out a phaseshift analysis of the relative angular distributions of electrons scattered from the $(1s2s^2)^2S$ state of helium and from the $(3s^23p^54s)^2P_{3/2}$, $^2P_{1/2}$ states of argon which can only decay into the elastic scattering channel. The measured phaseshifts are then coupled with accurate determinations of the ratio of beam densities of neon, krypton and xenon respectively, to helium and argon to yield absolute cross sections.

A number of calculations of the elastic differential scattering cross section of electrons from neon, krypton and xenon have been reported. Thompson (1966, 1971) has included both exchange and polarization effects in a single-state approximation calculation to predict the differential elastic scattering cross section for electrons from neon for electron energies up to 19·6 eV. Walker (1971) has calculated the differential elastic scattering cross sections for electrons from neon, krypton and xenon over a wide range of energies. His calculation is an exact numerical solution of the relativistic independent-particle model for scattering from the ground state of the atom. A similar calculation has also been carried out by Fink and Yates (1970), but exchange effects are neglected, whereas they were included in the calculations of Walker. The calculations of Berg *et al* (1971) use a simple analytic potential to describe the scattering. Khare and Shobha (1974) have calculated differential elastic scattering cross sections for electrons from neon in the plane-wave approximation, but their results lie outside the range of the present study.

The most obvious omission from all the above calculations is the coupling with inelastic channels. An attempt to include this effect has been made by Lewis *et al* (1974a) who used a semi-phenomenological optical-model calculation (Furness and McCarthy 1973).

Since none of the recent previous experimental measurements of the differential elastic scattering cross section satisfy conditions (i)–(iii) above, the nature and extent of recent previously published data is best summarized in tabular form (see table 1). In addition we are also aware of the unpublished absolute neon data of Preston (1972), and Andrick (private communication) and the normalized neon data of Jansen *et al* (private communication).

2. Experimental procedures

The apparatus, experimental procedures and cross section calibration techniques used in this study are the same as those already described in detail for studies of inelastic scattering of electrons from atomic hydrogen (Williams and Willis 1975b) and elastic scattering of electrons from argon (Williams and Willis 1975a). Hence a brief summary of these points is given here, emphasizing only those aspects of importance for the present measurements.

Table 1. Summary of the nature and extent of recently published differential elastic scattering cross sections for electrons from neon, krypton and xenon.

	Investigator	Energy range (eV)	Angular range (deg)	Comments
Ne	Mehr (1967)	30	20–155	Relative cross sections
	Schackert (1968)	40	40–150	Relative cross sections
	Kurepa *et al* (1973)	100–200	10–150	Absolute cross sections (from measured parameters)
	Bromberg (1974)	200–700	3–25	Absolute cross sections (from measured parameters)
	Lewis *et al* (1974a)	100	15–140	Normalized to optical-model calculations
	Gupta and Rees (1975)	100–625	10–150	Normalized (see text) and relative cross sections
Kr	Mehr (1967)	30	55–155	Relative cross sections
	Schackert (1968)	50–150	30–150	Relative cross sections
	Bromberg (1974)	200–700	3–25	Absolute cross sections (from measured parameters)
	Lewis *et al* (1974a)	30–200	15–140	Normalized to optical-model calculations
Xe	Mehr (1967)	20–300	20–155	Relative cross sections
	Schackert (1968)	50–150	30–150	Relative cross sections
	Bromberg (1974)	300–700	3–25	Absolute cross sections (from measured parameters)
	Lewis *et al* (1974a)	60	15–140	Normalized to calculations of Walker (1971)

2.1. Apparatus and experimental procedure

The apparatus and experimental procedures are based on the crossed electron and modulated atom beams technique first used by Fite and Brackmann (1958). Compared with earlier experiments by other workers using this technique, substantial improvements have been made in the electron beam optics and in the angular resolution and momentum selection of both the incident and scattered electrons.

In the present experiments the atom beam issued from a furnace (at room temperature) previously used as a source of atomic hydrogen. The beam was 100 % modulated and crossed a beam of electrons from an electron gun incorporating a 127° electrostatic monochromator. At 40 eV, for example, the incident electron beam had a beam angle less than 0·5°, a pencil angle of 0·75° and a beam diameter of 0·5 mm at a current of 1×10^{-7} A. These characteristics showed little variation outside that required by the Helmholtz–Lagrange relations over the entire range of the present studies.

Extensive electrostatic and magnetic shielding allowed the scattering to take place in an essentially field-free interaction region. The scattered electrons were analysed in either of two identical 127° electrostatic momentum analysers. After energy analysis, the scattered electrons were detected using a channel electron multiplier in conjunction with single-pulse counting and digital data recording techniques.

The two modes of operation of the scattered electron analysers described by Williams and Willis (1975b) were again used in this work. These modes were (*a*) a high-resolution mode with the energy resolution set at 32 meV from which the total scattered current in

either an elastic or inelastic scattering peak is obtained by scanning the analyser transmission energy across the peak and integrating under the peak and (*b*) a high-transmission mode in which the analyser is operated with a wide energy pass band such that a flat-topped transmitted-beam profile is obtained. The former mode was necessarily used during calibration for observation of the resonances while most of the non-resonant elastic scattering data were obtained with mode (*b*) analyser operation. At all energies angular distribution data were obtained with both modes of operation to ensure the reliability of the measurements.

The energy scales were calibrated by determining (i) the energies of the $^2P_{3/2}$, $^2P_{1/2}$ resonances for each rare gas studied and (ii) from the onsets of Ne^+, Kr^+ and Xe^+ production. These calibrations have yielded energy scales accurate to $\pm 0{\cdot}1$ eV.

The angular resolution of the scattered-electron analyser (including input optics) was estimated from geometrical considerations to be 1·5 degrees. Our differential elastic scattering studies in argon (Williams and Willis 1974, 1975a) showed that it was not possible to improve the data using higher angular resolutions. Then our approach was to change the dimensions of the beam angular acceptance slits of the analyser, such that estimated angular acceptances of 5, 4, 3, 2, 1·5, 1·0 and 0·5 degrees were available. We found that the depth of the minimum at 40 eV and 68° decreased as the angular acceptance decreased down to 1·5 degrees. For 1·0 and 0·5 degree angular acceptances, the depth of the minimum was unchanged from that measured for 1·5 degrees. Our methods of measurement did not permit us to determine whether this limitation was set by the fact that we had observed the true depth and width of the angular dip or by an instrumental effect, such as an aberration. Similar observations, and conclusions, were obtained for the dip at 128 degrees and 40 eV scattering energy.

The use of two analysers (detectors) of the scattered electrons greatly facilitated the rate of data acquisition and enabled the ratio of cross sections at two scattering angles to be measured simultaneously. This facility was also useful in establishing the absence of any asymmetries in the angular distributions between $+\theta$ and $-\theta$.

In the present experiments, the crossed electron and modulated atom beam technique provides an efficient and accurate method of eliminating background signal. This is particularly important if accurate cross sections are to be obtained in the region of deep cross section minima where the true scattered signal is relatively small.

2.2. Cross section calibrations

2.2.1. Relative calibration. The elastic differential cross section, $I(k, \theta)$, per element of solid angle, $d\Omega$, at a scattering angle θ, and electron wavenumber, k, (equal to $E^{1/2}$ in rydbergs) is given by

$$I(k, \theta)\, d\Omega = N(k, \theta)\, d\Omega \left(\int_\tau \int_\Omega J_e(x, y, z, k) n(x, y, z) \epsilon(x, y, z, k, \theta, \phi)\, d\Omega\, d\tau \right)^{-1} \tag{1}$$

where $N(k, \theta)\, d\Omega$ is the number of elastically scattered electrons per unit time into solid angle $d\Omega$; $J_e(x, y, z, k)$ is the incident electron-beam flux in the interaction volume $d\tau$; $n(x, y, z,)$ is the density of the target atoms which have a velocity distribution $f(V)$ in the interaction volume $d\tau$; $\epsilon(x, y, z, k, \theta, \phi)$ is a relative cross section calibration function which represents the non-ideal behaviour of the apparatus. The terms inside the large brackets are referred to collectively as the beam overlap integral, although the term (as defined above) will contain factors (described later) which pertain only to $N(k, \theta)$. The

determination of relative (and absolute) cross section values is made difficult by the need to monitor (and measure) the quantities in equation (1) at all times during the measurements.

The atom flux, J_a, is defined by the relationship

$$J_a(x, y, z) = \int n(x, y, z) f(V)\, dV.$$

By scanning the square cross section atom beam in the y and z directions (that is normal to the axis of the atom beam) it was indicated that n was constant across the beam. It was assumed that the atomic beam had a mean velocity, V_m, and then $J_a = nV_m$. Because an absolute detector of ground-state rare-gas atoms is not available, it is not possible to measure in absolute terms those parameters relating to the atom density. However, it can be arranged that the density of the atomic beam remains constant during the experiments. Two independent methods were used to ensure a constant atom density during the present measurements. Firstly, the intensity of rare-gas ions (X^+) emerging from an ionization-type detector, (electron-impact ionization followed by mass analysis with a quadrupole mass filter) placed with its axis along the atom beam direction, was monitored. Secondly, the pressure due to rare-gas atoms was measured in the gas supply line. This pressure ($\sim 0{\cdot}3$ Torr) was monitored by a simple manometer using low-vapour-pressure oil. The outputs of each of these two monitors were obtained as analogue voltage signals that were fed into comparator circuits which, in turn, could stop data recording if the monitor signal deviated by more than 2 % from a preset level.

The term $J_e(x, y, z, k)$ for the incident electron beam was continuously monitored by a Faraday cup zonal collector during the measurements and was probed during the setting up procedures by the Faraday cup and by the 127° electrostatic momentum analyser. The combination of the two detectors allowed the following aspects of the electron beam to be probed: the total beam flux, the flux density, the energy, the angular and energy spread at ten equidistant intervals across the beam diameter. At each beam energy, the dependence of J_e upon its parameters was always determined.

The function $\epsilon(x, y, z, k, \theta, \phi)$ contains many factors to allow for effects such as (i) variation of analyser solid angle of acceptance with change of scattering angle, energy and interaction volume, (ii) transmission of analyser and lenses at various scattering angles and energies, (iii) detector efficiency for various electron energies and incident electron fluxes and (iv) small changes in electron beam optics over the incident energy range of 20 to 400 eV. In order to establish the magnitude and form of such factors, which establish the experimental accuracy, all the pertinent measurements have been rigorously carried out (Williams and Willis 1975b).

The result of all the above considerations is that only the atomic beam velocity, V, was assumed constant. The dependence of each of the other terms upon its variables was established experimentally. A numerical integration was made at each k to establish the relative values of the differential cross section.

2.2.2. Absolute cross section calibration. The absolute cross section calibration was made by a phaseshift analysis of the relative angular distributions of electrons elastically scattered from a resonant state whose only mode of decay is the incident elastic channel. This method is described by Williams and Willis (1975b) for the 19·35 eV $(1s2s^2)^2S$ resonant state of helium and by Williams and Willis (1975a) for the 11·10 and 11·27 eV $(3s^23p^54s^2)^2P_{3/2}$ and $^2P_{1/2}$ resonant states of argon. In each case the phaseshifts determined lead to an absolute value of the differential elastic scattering cross section at

the resonance energy. Hence, in equation (1) absolute values have now been determined for the elastic differential cross section (in helium and argon at the resonances energies), the scattered electron current and all the other terms except the beam density, for which an absolute value can now be evaluated in each case. Further, the source pressure gauge can then be calibrated in terms of this beam density.

It was also shown (*a*) that the source pressure p was directly proportional to the scattered signal intensity for both helium and argon and then (*b*) that the ratio of helium to argon beam flux densities was given, at low values of p, by

$$\frac{J_{He}}{J_{Ar}} = \frac{p_{He}}{p_{Ar}}\left(\frac{M_{Ar}}{M_{He}}\right)^{1/2}$$

which arises from the relation

$$J = 1{\cdot}115 \times 10^{22} p A_s d^{-2} (MT)^{-1/2}$$

where J is the forward intensity per unit area (in $cm^{-2}\ s^{-1}$) of gas atoms of mass M and temperature T effusing from a circular aperture of area A_s in a tube of pressure p at a distance d from the source (Ramsey 1956).

From this evidence it was concluded that the density of other atom beams (in this case neon, krypton and xenon) could be deduced from measurements of the source pressure. To measure an absolute value of a differential elastic cross section in say, helium, at an energy and angle different from that used for the calibration, it is a necessary and sufficient measurement to establish the relative change in each of the terms in the beam overlap factor of equation (1) rather than to determine separate absolute values. Further, when the target gas is changed, it is necessary to establish the dependence of all parameters in equation (1) on the nature of the target gas. All parameters were independent of the target gas. However, on changing the target gas, it was found necessary to retune the incident electron monochromator to optimize the electron current at a particular energy.

The errors arising as a result of the relative and absolute cross section calibrations are quoted for each cross section value in the next section. The method of estimation has previously been discussed in detail by Williams and Willis (1975b).

3. Results and discussion

3.1. Neon

The absolute differential elastic cross sections obtained for the scattering of electrons from neon atoms for incident electron energies in the range 20–200 eV and for scattering angles from 20–150 degrees are presented in table 2. The 100 eV data is also compared with previous measurements and calculations in figure 1.

At 200 eV, the angular distribution shows a broad minimum centred around a scattering angle in the region of 90°, perhaps indicating dominant p-wave scattering. At lower electron energies, the minimum moves to higher scattering angles ($\theta = 120°$ at 20 eV), suggesting that the influence of a larger number of interfering partial waves must be considered.

The absolute cross sections measured by Preston (1972) for $20° \leqslant \theta \leqslant 90°$ and electron energies up to 100 eV were obtained from phaseshift determinations carried out at 19·1 eV in helium. Their angular distributions indicate relatively fewer electrons

Table 2. Elastic differential cross sections (in $a_0^2\,sr^{-1}$) for the scattering of electrons from neon atoms. The numbers in brackets indicate the possible error in the least significant digits in the cross section, for example, at 50 eV and 108°, the cross section is $0{\cdot}0148 \pm 0{\cdot}0014$ $a_0^2\,sr^{-1}$.

Angle (deg) \ Energy (eV)	20	30	40	50	100	200
15	—	—	—	—	—	4·31(48)
20	1·83(21)	1·90(20)	2·35(26)	2·67(28)	4·70(52)	2·89(30)
25	—	—	—	—	3·35(40)	1·92(22)
30	1·87(22)	1·87(19)	1·98(22)	2·13(23)	2·49(27)	1·26(14)
35	—	—	—	—	1·58(17)	0·863(102)
40	1·91(21)	1·77(19)	1·55(17)	1·72(19)	1·20(13)	0·580(71)
50	1·88(22)	1·65(18)	1·47(16)	1·35(14)	0·672(77)	0·297(32)
60	1·74(19)	1·43(15)	1·16(13)	1·06(12)	0·408(46)	0·177(19)
70	1·49(15)	1·12(12)	0·853(98)	0·778(82)	0·236(26)	0·118(13)
80	1·13(13)	0·796(80)	0·539(63)	0·419(43)	0·119(13)	0·0974(100)
90	0·753(88)	0·458(51)	0·282(31)	0·156(17)	0·0480(54)	0·102(11)
92	—	—	—	—	0·0375(43)	—
94	—	—	—	—	0·0346(36)	—
96	—	—	—	—	0·0325(34)	—
98	—	—	—	—	0·0327(35)	—
100	0·472(53)	0·226(25)	0·101(11)	0·0291(34)	0·0378(39)	0·113(14)
102	—	—	—	0·0205(23)	0·0471(52)	—
104	—	—	0·0682(74)	0·0182(20)	—	—
106	—	0·162(18)	0·0645(72)	0·0161(17)	—	—
108	—	0·149(17)	—	0·0148(14)	—	—
110	0·268(27)	0·143(16)	0·0768(87)	0·0217(23)	0·103(13)	0·138(16)
112	—	0·148(17)	—	0·0413(47)	—	—
114	—	0·157(17)	—	0·0824(86)	—	—
116	—	0·174(19)	—	—	—	—
118	—	0·191(22)	—	—	—	—
120	0·236(25)	0·236(26)	0·251(28)	0·229(24)	0·279(31)	0·176(19)
130	0·390(44)	0·539(61)	0·633(67)	0·636(69)	0·454(49)	0·235(25)
140	0·662(71)	0·930(113)	1·02(13)	1·18(13)	0·726(81)	0·274(30)
150	0·861(90)	1·45(16)	1·49(16)	1·87(21)	0·992(117)	0·317(35)

scattered into small angles compared with $\theta = 90°$ than is the case in the present experiment. This was also true of their argon data (Williams and Willis 1975a). It does not appear that the discrepancy can be explained in terms of the lower angular resolution used by Preston and in view of the more rigorous experimental tests reported here, one is forced to conclude that their collection efficiency was not completely independent of angle. In general, the absolute values of their cross sections lie below the present values, the degree of discrepancy differing for different electron energies. The 100 eV data (figure 1) represent the worst case, with their cross section at 20° lying more than a factor of five below the present value.

The present data at small scattering angles is in agreement with the recent absolute cross section measurements of Bromberg (1974). His data, obtained by absolute measurement of all the parameters involved in the scattering process, agrees with the present at 200 eV to within the combined experimental uncertainties.

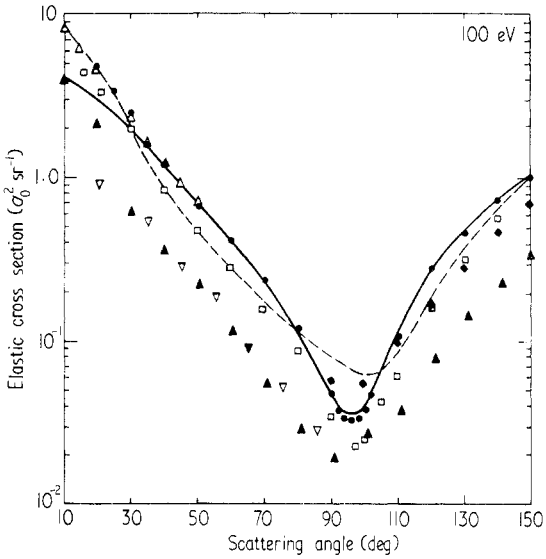

Figure 1. Differential cross sections for the elastic scattering of 100 eV electrons from neon atoms. ● present absolute measurements; □ normalized cross sections of Lewis *et al* (1974a); full curve, relativistic exchange calculations of Walker (1971); broken curve, optical-model calculations of Lewis *et al* (1974a); unless otherwise specified these notations are also used in figures 2–5. Other notations are: ▽ absolute cross sections of Preston (1972) and ▲ Kurepa *et al* (1973); ◆ normalized cross sections of Gupta and Rees (1975) (for angles $\leqslant 80°$ their data points overlap the present) and △ Jansen *et al* (private communication).

The data of Andrick (private communication) at 20 eV shows general agreement in shape with the present data at 20 eV, although there are indications of slight deviations at the extremities of the angular range. The absolute values of the cross section also show reasonable agreement, the discrepancy never exceeding 18%. The absolute cross sections of Kurepa *et al* (1973), obtained by measurement of all pertinent experimental parameters, agrees quite well in shape with the present data at 100 eV but less well at 200 eV where they indicate relatively more electrons scattered through small angles compared with 90°. At both energies their absolute cross section values lie well below the present, the discrepancy being almost an order of magnitude at 200 eV.

Differential cross sections have very recently been reported by Gupta and Rees (1975). In the energy range which overlaps the present data, namely 100–200 eV, their cross sections were obtained using a helium–neon gas mixtures method followed by normalization of their angular distributions to eikonal Born series calculations of Byron and Joachain (1973) in helium. At both 100 eV and 200 eV their data show good agreement with the present for angles less than 80°. At higher angles their data generally fall below the present curves, although their 100 eV minimum is less shallow. Their helium data (Sethuraman *et al* 1974) show similar trends when compared with other measurements.

The cross sections of Jansen *et al* (private communication) at 100 and 200 eV for $\theta \leqslant 53{\cdot}5°$, obtained by normalization to the absolute differential elastic scattering cross sections for electrons from N_2 by Bromberg (1970) are in excellent agreement with the present results. At 100 eV, the data of Lewis *et al* (1974a), normalized to their optical-model calculations at 31·5°, show excellent agreement in shape with the present work. However, their cross section values lie consistently lower than the present by about

30 %. Their cross sections at 30, 40, 50 and 200 eV for $\theta = 30°$ are also consistently lower than the present, despite the fact that their corresponding optical-model calculations show good agreement with the present data. Justification for this normalization technique is based on the good agreement between their optical-model calculations (Lewis *et al* 1974b) and the absolute differential elastic scattering cross sections for electrons from argon at 40 and 50 eV measured by Williams and Willis (1974). Further comment upon their absolute values must be restricted in view of the variable parameters within their optical model, the full details of which have not been published for atoms other than argon.

The 30 eV angular distribution of Mehr shows the same general form as the present, although it appears as if their cross section is increasing much more rapidly at small angles. The 40 eV angular distribution of Schackert also shows reasonable agreement in shape with the present data. In both cases the depth of the minimum in the distribution is reduced.

At all energies, there is good agreement, both in shape and magnitude, between the theoretical cross sections of Walker (1971) and the present results. The only systematic discrepancy appears at small scattering angles where theory overestimates the cross section at low energies whereas it is underestimated at high energies. The much poorer agreement with experiment shown by the Fink and Yates (1970) calculation at 100 eV, presumably reflects the neglect of exchange in these calculations.

The optical-model calculations of Lewis *et al* (1974a) have previously been mentioned as a means of normalization of their experimental data. Despite the fact that they have included empirically the effect of inelastic processes taking place, their 100 eV calculation shows much less satisfactory agreement both in shape and magnitude with experiment than the calculations of Walker. At energies of 40, 50 and 200 eV and $\theta = 30°$, the optical-model calculation gives cross section values in better agreement with experiment than at 100 eV.

There is good agreement both in shape and magnitude with the theoretical curve of Thompson (1971) at 19·6 eV except at small angles.

3.2. Krypton

The absolute differential elastic scattering cross sections obtained for the scattering of electrons from krypton in the energy range 20–400 eV and over the angular range 20–150 degrees are presented in table 3. The 30 eV and 200 eV data are also shown in figures 2 and 3 respectively. At all energies the cross sections are characterized by the presence of deep minima. At lower electron energies, the minima are less pronounced and occur close to the angles of 54·7 and 125·3 degrees, where the square of the Legendre polynomials for pure d-wave scattering decreases to zero. However, it is obvious that as the energy is increased, the presence of three minima giving a distribution somewhat similar to the square of the third-order Legendre polynomial is indicative of f-wave scattering. The relative simplicity of the shape of the 400 eV cross section probably indicates the growing importance of higher-order partial waves and the interference between the different partial waves.

In the small region of overlap ($20° \leqslant \theta \leqslant 25°$) with the absolute data of Bromberg (1974), there is excellent agreement at 400 eV, but at 200 eV, Bromberg's cross section at 20° lies 36 % below the present value.

As in neon, the angular distributions of Lewis *et al* (1974a) agree well with the present distributions, particularly the angular positions of the maxima and minima in the cross

Table 3. Elastic differential cross sections (in $a_0^2\,sr^{-1}$) for the scattering of electrons from krypton atoms. The numbers in brackets indicate the possible error in the least significant digits in the cross section value, for example, at 40 eV and 50 degrees, the cross section value is $0{\cdot}806 \pm 0{\cdot}091\ a_0^2\,sr^{-1}$.

Angle (deg) \ Energy (eV)	20	30	40	50	100	200	400
20	41·7(4·6)	33·1(3·4)	31·5(3·4)	27·8(2·9)	18·6(2·1)	8·25(91)	3·40(35)
22	—	—	—	—	12·3(1·4)	—	—
24	—	—	—	—	8·92(97)	—	—
28	—	—	—	—	4·63(51)	—	—
30	27·9(3·1)	19·3(2·1)	14·4(1·6)	11·7(1·3)	2·95(34)	1·01(12)	1·12(13)
36	—	—	—	—	0·688(72)	—	—
38	—	—	—	—	0·358(40)	—	—
40	14·4(1·5)	7·38(82)	4·47(49)	2·12(23)	0·207(22)	0·762(82)	0·596(63)
42	—	—	—	—	0·158(17)	—	—
44	—	—	—	—	0·153(17)	—	—
46	—	—	—	—	0·240(26)	—	—
48	—	—	—	—	0·368(40)	—	—
50	5·95(62)	2·05(22)	0·806(91)	0·298(32)	0·566(61)	0·727(75)	0·318(34)
52	—	—	—	0·201(22)	—	—	—
54	—	—	—	0·213(26)	—	—	—
56	—	—	0·341(39)	0·257(27)	—	—	—
58	—	—	0·284(41)	—	—	—	—
60	2·06(22)	0·559(72)	0·259(33)	0·404(46)	1·08(15)	0·548(64)	0·117(14)
62	—	0·408(50)	0·247(26)	—	—	—	—
64	—	0·347(41)	0·263(29)	—	—	—	0·0750(89)
66	—	0·297(33)	0·315(39)	—	—	—	—
68	—	0·265(30)	—	—	—	—	—
70	0·657(68)	0·296(35)	0·450(54)	0·826(125)	1·09(14)	0·164(17)	0·0521(62)
72	0·567(71)	0·335(38)	—	—	—	0·115(13)	0·0519(70)
74	0·505(57)	—	—	—	—	0·0732(82)	0·0580(70)
76	0·532(62)	—	—	—	—	0·0383(42)	0·0668(74)
78	0·581(70)	—	—	—	—	0·0145(17)	—
80	0·633(73)	0·654(77)	—	0·972(133)	0·484(63)	0·00567(62)	0·0874(101)
82	—	—	—	—	—	0·00692(102)	—
84	—	—	—	—	—	0·00972(118)	—
86	—	—	—	—	—	0·0348(38)	—
88	—	—	—	—	—	0·0570(68)	—
90	1·08(14)	1·14(13)	0·796(95)	0·765(90)	0·0982(145)	0·0991(150)	0·116(13)
92	—	—	—	—	0·0657(73)	—	—
94	—	—	—	—	0·0583(69)	—	—
96	—	—	—	—	0·0506(62)	—	—
98	—	—	—	—	0·0465(57)	—	—
100	—	1·31(17)	0·720(78)	0·451(54)	0·0749(91)	0·327(35)	0·120(14)
102	—	—	—	—	0·113(14)	—	—
110	1·42(17)	1·28(15)	0·584(66)	0·218(24)	0·283(35)	0·358(39)	0·0953(115)
118	—	—	—	—	—	—	0·0447(52)
120	1·23(14)	1·00(14)	0·373(43)	0·0792(92)	0·405(48)	0·325(36)	0·0249(27)
122	—	—	—	—	—	—	0·0117(13)
124	—	—	—	—	—	—	0·00762(82)
126	—	—	—	—	—	—	0·00541(67)
128	—	—	0·219(23)	0·0266(29)	—	—	0·00673(77)
130	1·22(15)	0·615(72)	0·177(19)	0·0174(19)	0·352(40)	0·142(15)	0·00959(130)

Table 3.—continued

Angle (deg) \ Energy (eV)	20	30	40	50	100	200	400
132	—	—	0·133(16)	0·0116(15)	—	—	0·0158(17)
134	—	—	0·116(15)	0·0057(10)	—	—	0·0325(36)
136	—	—	0·0862(115)	0·0052(9)	—	0·0826(110)	0·0607(72)
138	—	—	0·0560(72)	0·0093(13)	—	0·0662(72)	0·0891(113)
140	1·65(19)	0·336(36)	0·0372(45)	0·0143(18)	0·170(21)	0·0593(75)	0·0993(122)
142	—	—	0·0215(24)	0·0258(29)	—	0·0676(82)	0·184(21)
144	—	—	0·0106(13)	0·0456(60)	—	0·0864(90)	0·265(27)
146	—	—	0·0061(9)	0·0747(92)	—	0·119(13)	0·337(36)
148	—	—	0·0038(11)	0·106(13)	—	0·181(21)	0·422(51)
150	2·70(29)	0·218(24)	0·0053(12)	0·144(17)	0·0457(56)	0·258(30)	0·572(64)

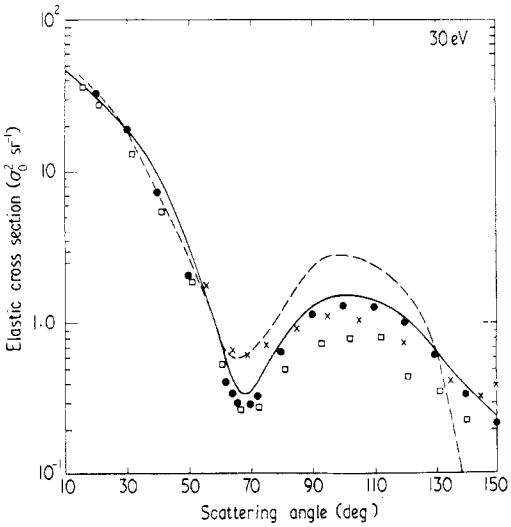

Figure 2. Differential cross sections for the elastic scattering of 30 eV electrons from krypton atoms. × relative cross sections of Mehr (1967) normalized to give best visual fit to present data.

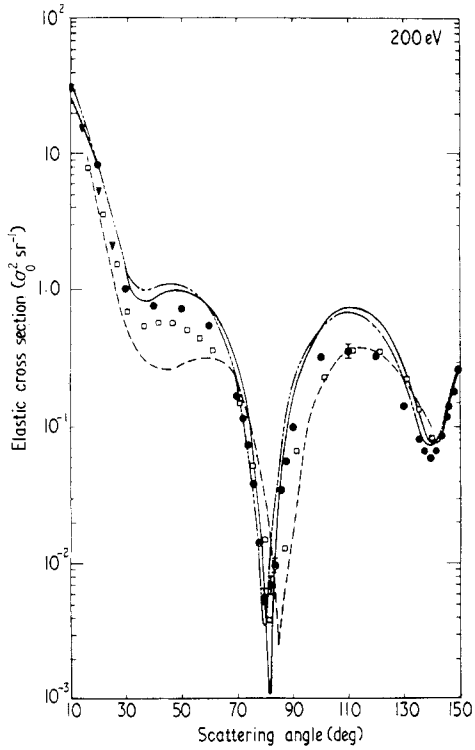

Figure 3. Differential cross sections for the elastic scattering of 200 eV electrons from krypton atoms. ▼ absolute cross sections of Bromberg (1974): chain curve, non-exchange calculations of Walker (1971).

sections. Discrepancies in the relative intensities at different angles do not appear to follow a particular pattern. Their cross sections, normalized to their optical-model calculations at 100 eV and $\theta = 31{\cdot}5°$ in krypton, also show general agreement with the

present work. It does appear, however, from the discrepancies between their data at 30 and 40 eV and $\theta = 30°$, and the present, that different energy dependencies of the differential cross section are obtained in the two experiments at low energies. This may be associated with the greater corrections which had to be applied to the data of Lewis *et al* for energies under 50 eV.

The angular distribution of Mehr at 30 eV shows the same general shape as the present results, but the depth of the cross section minima are much underestimated. The relative data of Schackert at 50 and 100 eV also show the same general form as the present.

The calculations by Walker include exchange effects for energies up to 200 eV. The theoretical curves agree well in shape with the experimental data, and compare well in magnitude with experiment at the lower energies, but significant discrepancies arise at the higher energies. For example, at 200 eV, the theoretical cross section minimum in the region of 80 degrees lies almost 80 % lower than the experimental value.

At 200 eV a calculation by Walker in which exchange is neglected is also shown in figure 3. This calculation shows better agreement in magnitude with experiment than the calculations in which exchange is included. If we again consider the 80 degrees minimum, the non-exchange cross section value lies less than 40 % below the experimental value. This observation is contrary to that in argon (Williams and Willis 1975a), where the inclusion of exchange in Walker's calculations showed a less marked effect at 200 eV and the exchange calculation was in better agreement with experiment, as one would expect. However there are deviations between theory and experiment in the positions of the minima so that a definite conclusion cannot be made about the preferred theoretical values either with or without exchange.

At 100 eV the calculation of Fink and Yates agrees well with that of Walker, as does the calculation of Berg *et al* (1971). Again the optical-model calculations of Lewis *et al* show greater deviations from experiment than those of Walker. In contrast to the expectations of Lewis *et al*, the discrepancies between the optical-model calculations and experiment are greatest at the highest energy, namely 200 eV.

3.3. Xenon

Table 4 shows the absolute differential elastic scattering cross sections for electrons with energies of 20–400 eV scattered from xenon through angles in the range 20–150 degrees. The 60 eV and 200 eV data are also presented in figures 4 and 5 respectively. As in the cases of argon (Williams and Willis 1974, 1975a) and krypton the dominant features of the distributions are the 'diffraction-pattern type' maxima and minima. At the lowest energies three comparatively shallow minima are observed. At intermediate energies four distinct minima can be seen, indicating the dominance of the $l = 4$ partial wave. As in krypton, some of the minima are not evident or become less pronounced at the higher energies, and obviously many partial waves are contributing to the observed results.

Again there is good agreement both in shape and magnitude of cross section with the exchange calculations of Walker, best agreement being obtained at the lower energies. At higher energies (200 eV and 400 eV), Walker's non-exchange theoretical curves successfully predict the correct form for the angular distributions although fairly large discrepancies exist between the theoretical and experimental values of the absolute cross section (almost a factor of 5 in the region of the 60 degrees minimum at 200 eV). A comparison of Walker's exchange and non-exchange calculations at 200 eV shows

Table 4. Elastic differential cross sections (in $a_0^2\,sr^{-1}$) for the scattering of electrons from xenon atoms. The numbers in brackets indicate the possible error in the least significant digits in the cross section, for example, at 60 eV and 56 degrees, the cross section value is $0{\cdot}0750 \pm 0{\cdot}0082\ a_0^2\,sr^{-1}$.

Angle (deg) \ Energy (eV)	20	30	60	125	200	400
20	79·6(9·3)	75·8(8·2)	9·25(99)	6·22(70)	4·17(39)	4·88(51)
24	—	—	3·88(42)	1·82(21)	—	—
30	40·2(4·8)	32·2(3·4)	1·28(14)	1·18(13)	2·39(25)	1·73(19)
34	—	—	0·440(48)	2·11(23)	—	—
40	14·7(1·6)	6·89(7·2)	0·198(21)	2·24(24)	1·41(14)	0·552(60)
46	—	1·32(17)	—	—	—	—
50	3·63(38)	0·441(52)	0·139(15)	1·19(12)	0·296(27)	0·212(23)
52	—	0·408(52)	—	—	0·185(20)	—
54	—	0·381(39)	—	—	0·0772(84)	—
56	1·67(16)	0·470(55)	0·0750(82)	0·332(38)	0·0344(35)	—
58	—	1·13(17)	0·0667(81)	0·153(16)	0·0128(16)	—
60	1·34(15)	1·81(22)	0·0656(69)	0·0547(60)	0·0110(12)	0·201(21)
62	1·28(11)	2·34(27)	0·0622(71)	0·0206(22)	0·0276(28)	—
64	1·27(13)	—	0·0605(65)	0·0143(15)	0·142(15)	—
66	1·23(11)	—	0·0606(67)	0·0325(33)	0·337(36)	—
68	1·33(15)	—	0·0720(84)	0·162(18)	—	—
70	1·50(17)	3·47(36)	0·0841(96)	0·301(29)	0·501(63)	0·267(29)
72	1·59(20)	—	0·0878(97)	—	—	—
74	—	—	0·0869(110)	—	—	—
76	—	—	0·0804(89)	—	—	—
78	—	—	0·0667(72)	—	—	—
80	1·65(18)	2·56(27)	0·0510(49)	0·881(90)	0·783(92)	0·140(18)
82	—	—	0·0296(37)	—	—	—
84	—	—	0·0136(16)	—	—	—
85	—	—	0·00693(75)	—	—	—
86	—	—	0·00520(58)	—	—	—
87	—	—	0·00463(49)	—	—	—
88	—	—	0·00847(91)	—	—	0·0250(27)
89	—	—	0·0245(30)	—	—	—
90	1·51(19)	0·968(127)	0·0366(40)	0·864(104)	0·490(57)	0·0103(11)
92	—	—	0·0819(90)	—	—	0·00584(92)
94	—	—	0·127(14)	—	—	0·00830(105)
96	—	0·385(40)	—	—	—	0·0145(19)
98	—	0·364(39)	—	—	—	—
100	1·12(12)	0·318(33)	0·451(49)	0·385(42)	0·0685(77)	0·0531(66)
102	—	0·435(47)	—	—	0·0429(49)	—
104	—	0·500(56)	—	—	0·0263(31)	—
106	—	—	—	0·109(14)	0·0215(24)	—
108	—	—	—	0·0752(86)	0·0275(32)	—
110	1·26(13)	1·06(13)	1·13(12)	0·0735(121)	0·0668(91)	0·223(26)
112	—	—	—	0·0467(49)	—	—
114	—	—	—	0·0620(115)	—	—
116	—	—	—	0·0931(97)	—	—
120	1·47(17)	1·27(15)	1·28(15)	0·163(23)	0·390(44)	0·317(42)
130	1·22(15)	0·739(76)	1·15(13)	0·216(24)	0·595(68)	0·218(28)
132	—	0·611(66)	—	—	—	—
134	—	0·308(34)	—	—	—	—
136	—	0·0792(88)	—	—	—	—

Table 4.—continued

Angle (deg) \ Energy (eV)	20	30	60	125	200	400
138	—	0·0235(25)	—	—	—	—
140	0·858(86)	0·0416(46)	0·197(22)	0·0736(84)	0·256(33)	0·0504(59)
142	—	0·323(37)	0·0934(99)	0·0419(45)	—	0·0315(38)
144	—	0·688(70)	0·0358(38)	0·0458(49)	—	0·0232(29)
145	—	—	0·0212(23)	—	—	—
146	—	1·34(14)	0·0300(29)	0·0795(82)	—	0·0257(29)
147	—	—	0·0836(79)	—	—	—
148	—	2·25(25)	0·159(18)	0·228(22)	—	0·0458(53)
150	0·277(28)	3·17(35)	0·377(40)	0·461(63)	0·0524(71)	0·0869(113)

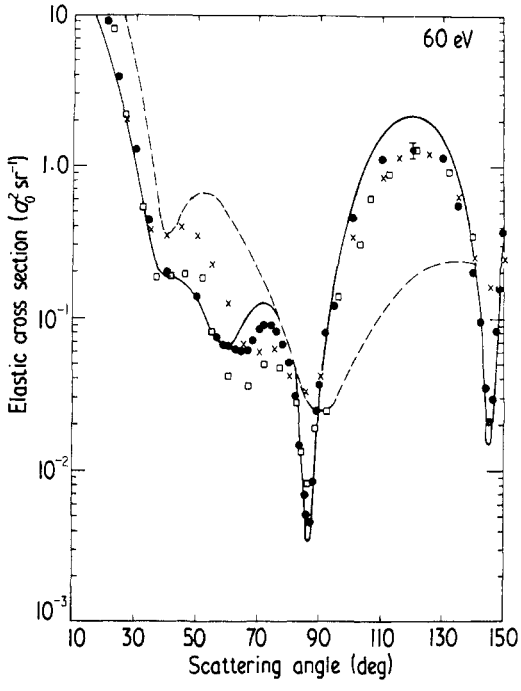

Figure 4. Differential cross sections for the elastic scattering of 60 eV electrons from xenon atoms. × relative cross sections of Mehr (1967) normalized to give best visual fit to present data.

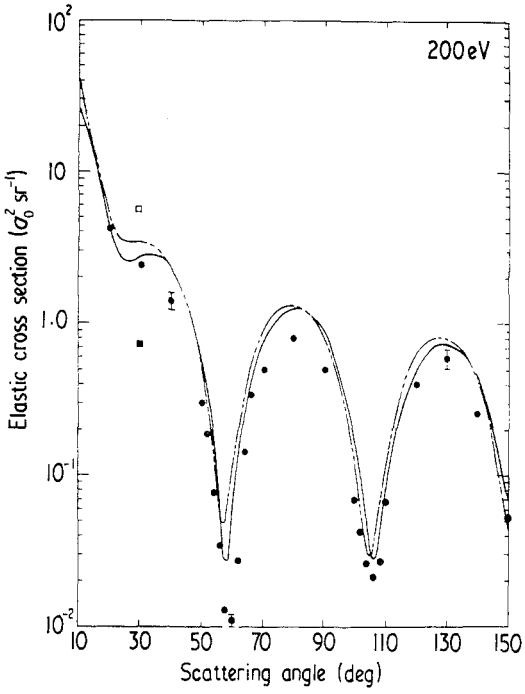

Figure 5. Differential cross sections for the elastic scattering of 200 eV electrons from xenon atoms. ■ optical-model calculation of Lewis *et al* (1974a); chain curve, non-exchange calculations of Walker (1971).

that the inclusion of exchange gives improved agreement with experiment, particularly in the region of the 60 degrees minimum.

At 60 eV (figure 4), the angular distribution of Lewis *et al* shows the same general shape as is obtained in the present experiment. Because Lewis *et al* have normalized their 60 eV data to that of Walker at 31·5°, their cross section values also agree well with

the present values. At 60 eV, the optical-model calculation of Lewis *et al* fails to predict both the form of the angular distribution and the magnitude of the differential cross section. Again their calculation at higher energies (125 and 200 eV for $\theta = 30°$) shows greater discrepancies with experiment, being more than an order of magnitude too low at 125 eV. Their experimental cross sections at 30 eV and 200 eV and $\theta = 30°$ lie a factor of 2 higher than the present, indicating, as in the case of krypton, the measurement of a different energy dependence for the differential cross section at this angle. At 400 eV and $\theta = 20°$, the cross section measured by Bromberg is 27% lower than the present value.

At 20 eV the angular distribution of Mehr shows little similarity with the present, especially for scattering angles greater than 120°. At 30 and 60 eV the agreement in shape is better but the data of Mehr grossly underestimate the depth of the cross section minima.

4. Conclusions

This paper presents absolute differential elastic scattering cross sections for the scattering of electrons from neon, krypton and xenon over a wide range of both electron energies and scattering angles and with high angular resolution. With high angular resolution it has been possible to obtain accurate angular distributions, particularly for krypton and xenon where sharp angular variations occur in the distributions. The angular distributions show good agreement with the recent high angular resolution work of Lewis *et al* and poor agreement with the distributions of other workers using lower angular resolutions, eg Mehr (1967) and Schackert (1968).

The magnitudes of the cross sections measured are not in consistent agreement with any previous data. In general the measured cross sections agree well with the calculations of Walker. The one apparent contradiction with Walker's calculations is the fact that his non-exchange calculation in krypton at 200 eV shows better agreement in magnitude with experiment than his exchange calculation. This is contrary to expectation and to observations in argon (Williams and Willis 1975a) and in xenon. It seems reasonable to conclude that the better agreement in the case of the non-exchange calculations in krypton is fortuitous and that this observation reflects the neglect of some other effects in the theory. The most obvious omissions are polarization and inelastic-channel coupling effects. The former would not be expected to be of great importance at this relatively high energy. The effect of the latter poses a theoretical problem which needs to be tackled.

The inclusion of inelastic coupling effects in optical-model calculations as performed by Lewis *et al* (1974a) yields cross sections in poorer agreement with experiment. In xenon their optical-model calculations fail to predict the correct shape for the angular distribution and the calculated values of the absolute cross section can be in error by more than an order of magnitude. Moreover the agreement with experiment does not appear to improve with increasing energy.

Acknowledgments

The authors are grateful to Dr D W Walker for supplying his data in tabular form and to the Science Research Council for financial support.

References

Berg R A, Purcell J E and Green A E S 1971 *Phys. Rev.* A **3** 508–10
Bromberg J P 1970 *J. Chem. Phys.* **52** 1243–7
—— 1974 *J. Chem. Phys.* **61** 963–9
Byron F W and Joachain C J 1973 *Phys. Rev.* A **8** 3266–9
Fink M and Yates A C 1970 *Atomic Data* vol 1 pp 385–456
Fite W L and Brackmann T R 1958 *Phys. Rev.* **112** 1141–51
Furness J B and McCarthy I E 1973 *J. Phys.* B: *Atom. Molec. Phys.* **6** 2280–91
Gupta S C and Rees J A 1975 *J. Phys.* B: *Atom. Molec. Phys.* **8** 417–25
Khare S P and Shobha P 1974 *J. Phys.* B: *Atom. Molec. Phys.* **7** 420–7
Kieffer L J 1971 *Atomic Data* vol 2 pp 293–392
Kurepa M V, Vuskovic L D and Klalezic S D 1973 *Proc. 8th Int. Conf. on Physics of Electronic and Atomic Collisions, Belgrade* (Belgrade: Institute of Physics) Abstracts pp 267–8
Lewis B R, McCarthy I E, Teubner P J O and Weigold E 1974a *J. Phys.* B: *Atom. Molec. Phys.* **7** 2549–56
—— 1974b *J. Phys.* B: *Atom. Molec. Phys.* **7** 1083–90
Massey H S W and Burhop E H S 1969 *Electronic and Ionic Impact Phenomena* vol 1 (London: Oxford University Press)
Mehr J 1967 *Z. Phys.* **198** 345–50
Preston J A 1972 *PhD thesis* The Queen's University of Belfast
Ramsey N F 1956 *Molecular Beams* (Oxford: Clarendon Press)
Schackert K 1968 *Z. Phys.* **213** 316–22
Sethuraman S K, Rees J A and Gibson J R 1974 *J. Phys.* B: *Atom. Molec. Phys.* **7** 1741–7
Thompson D G 1966 *Proc. R. Soc.* A **294** 160–74
——1971 *J. Phys.* B: *Atom. Molec. Phys.* **4** 468–82
Walker D W 1971 *Adv. Phys.* **20** 257–323
Williams J F and Willis B A 1974 *J. Phys.* B: *Atom. Molec. Phys.* **7** L51–55
—— 1975a *J. Phys.* B: *Atom. Molec. Phys.* **8** 1670–82
—— 1975b *J. Phys.* B: *Atom. Molec. Phys.* **8** 1641–69